Functionality of the Seventh and Eighth Transmembrane Domains of Acyl-Coenzyme A:Cholesterol Acyltransferase 1†

Zhan-Yun Guo,‡ Catherine C. Y. Chang, and Ta-Yuan Chang*

Department of Biochemistry, Dartmouth Medical School, Hanover, New Hampshire 03755

Received June 8, 2007; Revised Manuscript Received July 3, 2007

ABSTRACT: Acyl-coenzyme A:cholesterol acyltransferase 1 (ACAT1) is a resident enzyme in the endoplasmic reticulum. ACAT1 is a homotetrameric protein and contains nine transmembrane domains (TMDs). His460 is a key active residue and is located within TMD7. Human ACAT1 has seven free Cys, but the recombinant ACAT1 devoid of free Cys retains full enzyme activity. To further probe the functionality of TMD7 (amino acids 446−460) and TMD8 (amino acids 466−481), we used a parental ACAT1 devoid of free Cys as the template to perform Cys-scanning mutagenesis within these regions. Each of the single Cys mutants was expressed in Chinese hamster ovary (CHO) cell line AC29 lacking endogenous ACAT1. We measured the effect of single Cys substitution on enzyme activity and used the Cu(1,10-phenanthroline)$_2$SO$_4$-mediated disulfide cross-linking method to probe possible interactions of engineered Cys between the two identical subunits. The results show that several residues in one subunit closely interact with the same residues in the other subunit; mutating these residues to Cys does not lead to large loss in enzyme activity. Helical wheel analysis suggests that these residues are located at one side of the coil. In contrast, mutating residues F453, A457, or H460 to Cys causes large loss in enzyme activity; the latter residues are located at the opposite side of the coil. A similar arrangement is found for residues in TMD8. Thus, helical coils in TMD7 and TMD8 have two distinct functional sides: one side is involved in substrate-binding/catalysis, while the other side is involved in subunit interaction.

The enzyme acyl-coenzyme A:cholesterol acyltransferase (ACAT)[1] plays an important role in cellular cholesterol homeostasis. ACAT catalyzes the formation of cholesteryl esters, using cholesterol and long-chain fatty acyl coenzyme A as substrates (*1*). In mammals, two ACAT genes exist, encoding two different proteins, ACAT1 and ACAT2. The expression of ACAT1 is ubiquitous, while the expression of ACAT2 is tissue-restricted (*2*−*4*). Both enzymes are potential drug targets for therapeutic intervention against atherosclerosis and hyperlipidemia. ACAT1 is an integral membrane protein present in the ER, with a 50 kDa apparent molecular mass on SDS−PAGE. ACAT2 is also an integral membrane protein (*5*); it shares high homology with ACAT1 near the C-terminus but not near the N-terminus. The structural models of ACAT1 and related proteins are not currently available due to the difficulty of crystallizing membrane proteins.

Unlike many other enzymes/proteins involved in cellular cholesterol metabolism, ACAT1 is not regulated at the transcriptional level by the cholesterol-dependent SCAP/SREBP pathway (*6*). Instead, the activity of ACAT1 is allosterically activated by one of its substrates, cholesterol (*7*). There is also evidence to suggest that ACAT2 may be allosterically regulated by cholesterol (*8*). The molecular mechanism(s) that govern the allosterism of ACAT is unknown at present. Allosteric enzymes in general contain multiple interacting subunits. ACAT1, for example, is a homotetrameric enzyme (*9*) and contains nine transmembrane domains, with the active site (His 460) located within TMD7 (*10*). A hydrophilic segment near the N-terminus located on the cytoplasmic side of the ER membrane contains one dimerization domain, the deletion of which converts the enzyme to a fully functional homodimeric form (*11*). The second dimerization domain is unknown. We noted that the sequences present in TMD7 (aa 446−460) and TMD8 (aa 466−481) are rich in conserved residues. These residues may contribute to both substrate binding/catalysis and to subunit interaction. To test this hypothesis, in this work we performed cysteine-scanning mutagenesis experiments. We then performed enzyme activity measurements to analyze the effects of single Cys substitution at various positions within TMD7 and TMD8. We also used the Cu(1,10-phenanthroline)$_2$SO$_4$-(CuP-) mediated oxidative disulfide cross-linking strategy

† This work was supported by NIH Grant HL60306 to T.-Y.C.

* To whom correspondence should be addressed: phone 603-650-1622; fax 603-650-1128; e-mail Ta.Yuan.Chang@dartmouth.edu.

‡ Present address: Institute of Protein Research, Tongji University, Shanghai, China.

[1] Abbreviations: aa, amino acids; ACAT, acyl-coenzyme A:cholesterol acyltransferase; AMS, 4-acetamido-4′-maleimidylstilbene-2,2′-disulfonic acid; CuP, Cu(1,10-phenanthroline)$_2$SO$_4$; CHO, Chinese hamster ovary; DMEM, Dulbecco's modified Eagle's medium; DMSO, dimethyl sulfoxide; dpm, disintegrations per minute; EDTA, ethylenediaminetetraacetic acid, ER, endoplasmic reticulum; FBS, fetal bovine serum; HRP, horseradish peroxidase; IgG, immunoglobulin; IA, iodoacetamide; NEM, *N*-ethylmaleimide; NPM, *N*-phenylmaleimide; PBS, phosphate-buffered saline; PEG-mal, poly(ethylene glycol)$_{5000}$−maleimide; PVDF, poly(vinylidene difluoride; SDS−PAGE, sodium dodecyl sulfate−polyacrylamide gel electrophoresis; SREBP, sterol response element binding protein; SCAP, sterol response element binding protein (SREBP) cleavage activating protein; TMD, transmembrane domain; Tris-HCL, tris(hydroxymethyl)aminomethane hydrochloride; WT, wild type.

10.1021/bi7011367 CCC: $37.00
Published on Web 08/11/2007

(*12*−*14*) to probe possible interactions between the two TMD7s, and the two TMD8s. The results suggest that TMD7 and TMD8 may fulfill two distinct functions: several residues on one side of the coils form the interface for close interactions between the two adjacent TMDs, while several other residues, all located at the opposite side of the coils, are involved in enzyme catalysis and/or in substrate binding.

EXPERIMENTAL PROCEDURES

Materials

1,10-Phenanthroline, cupric sulfate ($CuSO_4$), *N*-ethylmaleimide (NEM), *N*-phenylmaleimide (NPM), iodoacetamide (IA), and methyl-β-cyclodextran were from Sigma. $MPEG_{5000}$-maleimide (PEG-mal) was from Watershears; 4-acetamido-4′-maleimidylstilbene-2,2′-disulfonic acid (AMS) was from Molecular Probes. Cu(1,10-phenanthroline)$_2SO_4$ (CuP) was prepared as a stock solution (20 mM) in 50 mM Tris-HCl (pH 7.8) from cupric sulfate and 1,10-phenanthroline with a molar ratio of 1/2 (*13*, *14*). AMS, NEM, and NPM were freshly prepared as stock solutions (80 mM) in dimethyl sulfoxide (DMSO). PEG-mal was freshly prepared in 10% SDS, 50 mM Tris-HCl, and 1 mM EDTA (pH 7.5). FuGENE 6 transfection reagent was from Roche. [9,10-$^3H_2$]Oleic acid was from Amersham Pharmacia Biotech. PVDF membrane (Immobilon P) was from Millipore. Rabbit polyclonal antibodies (DM10) generated against the N-terminal fragment (1−131) of hACAT1 were described previously (*15*). Goat anti-rabbit IgG(L+H)−HRP conjugate and goat anti-mouse IgG(L+H)−HRP conjugate were from Bio-Rad. SuperSignal West pico chemiluminescent substrate was from Pierce.

Methods

Recombinant DNA Technology. The ACAT1 mutants with a single engineered free Cys were constructed by using the Quik-Change II XL mutagenesis kit from Stratagene according to manufacturer's manual. The DNA construct pcDNA3/[C2(528/546)]His-hACAT1 (*16*) was used as the mutagenesis template. The expected mutations were all confirmed by DNA sequencing.

Cell Culture. Unless otherwise indicated, CHO cells were cultured in medium A [F-12/DMEM (50:50) supplemented with 10% fetal bovine serum] in a 5% CO_2 incubator at 37 °C. The ACAT1-deficient CHO cell line AC29 (*17*) was used to express the ACAT1 mutants. For transfections, the AC29 cells were cultured in 6- or 12-well plates to 70−80% confluency and transfected with 2 μg of pcDNA3 vectors encoding various ACAT1 mutants by use of the FuGENE 6 transfection reagent. For ACAT enzyme activity and protein expression studies, 1 day after transfection the cells were trypsinized, divided equally into three wells in 12-well plates, grown for 2 days in medium A containing G-418 (0.3 mg/mL), and then subjected to enzyme and protein expression studies. For disulfide cross-linking studies, 1 day after transfection the cells were trypsinized, pooled to a single 100 mm dish, and grown for 2 days at 37 °C in medium A with G418. To study the effect of cholesterol content on disulfide cross-linking efficiency, the transfected cells were grown in medium A for 2 days and then grown either in cholesterol-rich medium [medium A plus 40 μM cholesterol complexed with methyl-β-cyclodextran (mol/mol = 1:10)] or in cholesterol-poor medium [F-12/DMEM (50:50) supplemented with 10% delipidated fetal bovine serum plus 35 μM oleic acid, 230 μM mevalonate, and 50 μM mevinolin (*18*)] for 24 h. Microsomes were prepared from these cells and subjected to disulfide cross-linking studies.

ACAT Activity Assay in Intact Cells. The method for measuring the rate of [^{3}H]cholesteryl oleate synthesis in intact cells as described previously (*19*) was employed. Cells were grown in medium A. They were given a fresh medium change (0.5 mL/well) 2 h before the assay began. To start the assay, 20 μL of 10 mM [^{3}H]oleate in 10% bovine serum albumin was added to the medium at 37 °C for 30 min. The formation of [^{3}H]cholesteryl oleate was quantitated by scintillation counting after lipid extraction and separation by thin-layer chromatography (*19*).

ACAT1 Protein Content Analysis after Transfection. The cells in 12-well plates were washed with 1 mL of PBS and lysed by 240 μL of lysis buffer (10% SDS and 50 mM Tris-HCl, pH 8.7) containing 10 mM iodoacetamide. The cell lysates were transferred to Eppendorf tubes, 60 μL/tube SDS−PAGE loading buffer (10% SDS, 20% glycerol, 0.05% bromophenol blue, and 50 mM Tris-HCl, pH 6.8) was added, and the samples were mixed by vigorous vortexing. Then 60 μL of the sample mixture were loaded onto an SDS−9% polyacrylamide gel. After electrophoresis, the proteins were transferred to a PVDF membrane, and the ACAT1 protein bands were visualized with anti-ACAT1 antibodies DM10 as the primary antibodies. The relative content of mutant hACAT1 versus WT hACAT1 was analyzed by densitometry.

CuP Oxidized Disulfide Cross-Linking. The AC29 cells transiently expressing various engineered ACAT1 mutants were lysed by hypotonic shock and scraping (*20*). The nuclei and intact cells were removed by centrifugation (4 °C, 800*g*, 5 min). Then, the microsomes in the 800*g* supernatant were precipitated by ultracentrifugation (4 °C, at 100 000*g* for 20 min) and gently resuspended in cold 50 mM Tris-HCl, pH 7.8. The microsomes were treated with CuP at a final concentration as indicated at 0 °C for 2 h. Next, EDTA stock solution (final concentration 30 mM) and NEM stock solution (final concentration 30 mM) were added to quench the cross-linking reaction; the reaction mixtures were continuously incubated at 0 °C for 1 h. Afterward, 10% SDS stock solution was added at 3% final concentration. The mixture was incubated at room temperature for 30 min. Finally, $^1/_4$ volume SDS−PAGE loading buffer (10% SDS, 20% glycerol, 0.05% bromophenol blue, and 50 mM Tris-HCl, pH 6.8) was added. An appropriate amount of the reaction mixture was loaded onto an SDS−8.5% polyacrylamide gel. After electrophoresis, the proteins were transferred to a PVDF membrane, and the ACAT1 protein bands were visualized by western blot with anti-ACAT1 antibodies DM10 as the primary antibodies.

AMS, NEM, and NPM Modifications. Whole-cell homogenates were prepared by lysing the cells with hypotonic shock and scraping. The nuclei and unbroken cells were removed by centrifugation at 800*g* for 5 min at 0 °C. The 800*g* supernatants containing the microsomes were treated with AMS, NEM, or NPM as indicated at 0 °C for 1 h. The final concentration of AMS, NEM, or NPM was 4 mM. The reactions were carried out in buffer A (50 mM Tris-HCl and 1 mM EDTA, pH 7.8) with 5% DMSO. After incubation,

2-mercaptoethanol was added at 5 mM final concentration at 0 °C for 30 min (to react with the excess modification reagents). For samples not treated with any modification reagent, 2-mercaptoethanol was added at 2 mM concentration. Then an equal volume of lysis buffer (10% SDS in 50 mM Tris-HCl and 1 mM EDTA, pH 7.5) containing 10 mM PEG-mal was added to each sample and incubated at room temperature for 30 min, as described previously (*16*). The mixtures were analyzed by SDS−PAGE; the proteins were transferred to a PVDF membrane after electrophoresis. The ACAT1 bands were visualized by western blot with DM10 as the primary antibodies.

RESULTS

Determining the Enzyme Activities of Engineered Single Cys ACAT1 Mutants. The strategy of oxidative disulfide cross-linking mediated by Cu(1,10-phenanthroline)$_2$SO$_4$ (CuP) (chemical structure shown in Figure 3A) has been used to map the interaction interface between two adjacent subunits of oligomeric membrane proteins (*12*, *14*). With CuP, one disulfide cross-linking can be formed between two free Cys but only if the sulfhydryl groups in these two Cys are adjacent to each other. For this purpose, wild-type ACAT1 is not suitable as the starting material because it contains seven free Cys and a single disulfide bond located near the C-terminus of the protein (*16*). A mutant ACAT1, designated as C2 ACAT1, was created by genetic engineering. C2 ACAT1 still contains the disulfide bond but contains no free Cys, and it remains enzymatically active (*16*). Here, to test the hypothesis that TMD7 (aa 446−460) and TMD8 (aa 466−481) may contribute to subunit interaction within the membrane, we used C2 ACAT1 as the template to carry out Cys-scanning mutagenesis within TMD7 and TMD8 (Figure 1). We then performed transient transfections and measured the ACAT enzymatic activities in the transfected cells. The results are presented as relative enzyme activities (Figure 2A), relative ACAT1 protein expression levels (Figure 2B), and normalized relative activities (Figure 2C), respectively. We classify the results in four classes. The first class includes mutants V459C, L468C, S469C, and P473C. Each of these mutants had extremely low protein expression levels (Figure 2B). Our earlier work suggested that mutating certain residues in ACAT1 may severely disturb the structural integrity that leads to rapid degradation of the ACAT1 enzyme in intact cells (*16*). Since the total enzyme activities (Figure 2A) and protein expression levels of these mutants were both extremely low, we could not calculate their normalized enzymatic activities; these uncertainties are indicated with asterisks in Figure 2C. These mutants were not further pursued. The second class includes mutants F453C, S456C, A457C, H460C, and F479C. Each of these five mutants had less than 10% of the activity of normal C2 ACAT1. The protein expression levels of mutants F453C, A457C, H460C, and F479C were essentially the same as that of normal C2 ACAT1, while the protein expression level of the S456C mutant was only approximately 30% of the normal C2 ACAT1. The third class includes mutants S446C, A447C, A448C, L450C, A451C, V452C, A454C, V455C, V458C, V466C, A467C, F471C, Y472C, V474C, L475C, F476C, V477C, L478C, M480C, and F481C. When compared to the C2 ACAT1, each of these 20 mutants was expressed at normal or near-normal levels (Figure 2B), and each had normal or near-normal enzymatic activity (Figure 2C). The fourth class includes only the M449C mutant. This mutant had protein expression at approximately 60% of normal C2 ACAT1 and had approximately 20% of normalized ACAT enzyme activity (Figure 2C).

CuP Oxidized Disulfide Cross-Linking. Cu(1,10-phenanthroline)$_2$SO$_4$ (CuP) is a hydrophobic oxidizing agent in which the cupric ion is chelated by two hydrophobic 1,10-phenanthroline moieties (Figure 3A). This reagent has been used to test the adjacency of two sulfhydryl moieties within the membrane bilayer, where the hydrophilic cupric ion by itself cannot enter (*13*, *14*). We carried out the oxidized disulfide cross-linking experiments at low temperature (0 °C), using microsomes from CHO cells that transiently express various mutant ACAT1s described in Figure 2 as the enzyme sources. The nonreducing SDS−PAGE system was used to analyze the results. In this system, the non-cross-linked ACAT1 migrates as a monomer around 54 kDa,[22] while the cross-linked ACAT1 migrates as a dimer around 108 kDa. The cross-linking results are reported in Figure 3C. Each construct is studied in three lanes: the first lane was without CuP, the second lane was with 1 mM CuP, and the third lane was with 3 mM CuP. We developed a semiquantitative method to calculate the percent cross-linking; this method is explained in Figure 3B. The calculated percent dimer formation after treatment with 3 mM CuP is listed at the bottom of each construct (Figure 3C). For normal C2(528/546) hACAT1 (serving as the negative control), there is no detectable disulfide cross-linking between the two subunits. For single Cys ACAT1s within TMD7, the A447C, A451C, V455C, and V458C mutants formed a significant level of dimers with CuP (∼10% or higher of the total ACAT1 signal). The other four mutants, S446C, A457C, A448C, and V452C, also formed dimers but much less efficiently (1−4% of total signal). For single Cys ACAT1s within TMD8, only the V466C, A467C, F470C, V474C, and V477C mutants formed a significant level of dimers. Other mutants exhibited dimer formation much less efficiently or exhibited no dimer formation at all.

Locations of Reactive Cys within TMD7 and TMD8. The results described in Figure 3C show that only a limited number of engineered Cys are reactive to CuP catalyzed cross-linking, suggesting that these reactive Cys in one subunit are adjacent to their corresponding Cys in the other subunit. We analyzed the cross-linking results in terms of a helical wheel model (Figure 4A). The results show that when TMD7 is placed as a helical wheel, the four reactive residues (A447C, A451C, V455C, and V458C) are all located at the same side of the coil. These residues may form the interaction surface between two adjacent TMDs. The helical wheel analysis also shows that the other four mutants, S446C, A457C, A448C, and V452C, which formed cross-linked dimers less efficiently (1−4%), are located at the two edges of the putative interaction surface formed by the A447, A451, V455, and V458 residues. Other engineered mutants within TMD7 that did not form detectable disulfide cross-linking are all located on the opposite side of the putative interaction surface, as shown in Figure 4A. The same analysis shows

[2] C2 ACAT2 contained a 6×His tag at the N-terminus (*16*), rendering its apparent molecular mass to be 54 kDa, which is slightly larger than that of untagged ACAT1 (50 kDa).

A

```
1           11          21          31          41          51
MVGEEKMSLR NRLSKSRENP EEDEDQRNPA KESLETPSNG RIDIKQLIAK KIKLTAEAEE

61          71          81          91          101         111
LKPFFMKEVG SHFDDFVTNL IEKSASLDNG GCALTTFSVL EGEKNNHRAK DLRAPPEQGK

121         131         141         151         161         171
IFIARRSLLD ELLEVDHIRT IYHMFIALLI LFILSTLVVD YIDEGRLVLE FSLLSYAFGK

181         191         201         211         221         231
FPTVVWTWWI MFLSTFSVPY FLFQHWATGY SKSSHPLIRS LFHGFLFMIF QIGVLGFGPT

241         251         261         271         281         291
YVVLAYTLPP ASRFIIIFEQ IRFVMKAHSF VRENVPRVLN SAKEKSSTVP IPTVNQYLYF

301         311         321         331         341         351
LFAPTLIYRD SYPRNPTVRW GYVAMKFAQV FGCFFYVYYI FERLCAPLFR NIKQEPFSAR

361         371         381         391         401         411
VLVLCVFNSI LPGVLILFLT FFAFLHCWLN AFAEMLRFGD RMFYKDWWNS TSYSNYYRTW

421         431         441         451         461         471
NVVVHDWLYY YAYKDFLWFF SKRFKSAAML AVFAVSAVVH EYALAVCLSF FYPVLFVLFM
                        TMD7                    TMD8

481         491         501         511         521         531
FFGMAFNFIV NDSRKKPIWN VLMWTSLFLG NGVLLCFYSQ EWYARRHCPL KNPTFLDYVR

541         550
PRSWTCRYVF
```

B

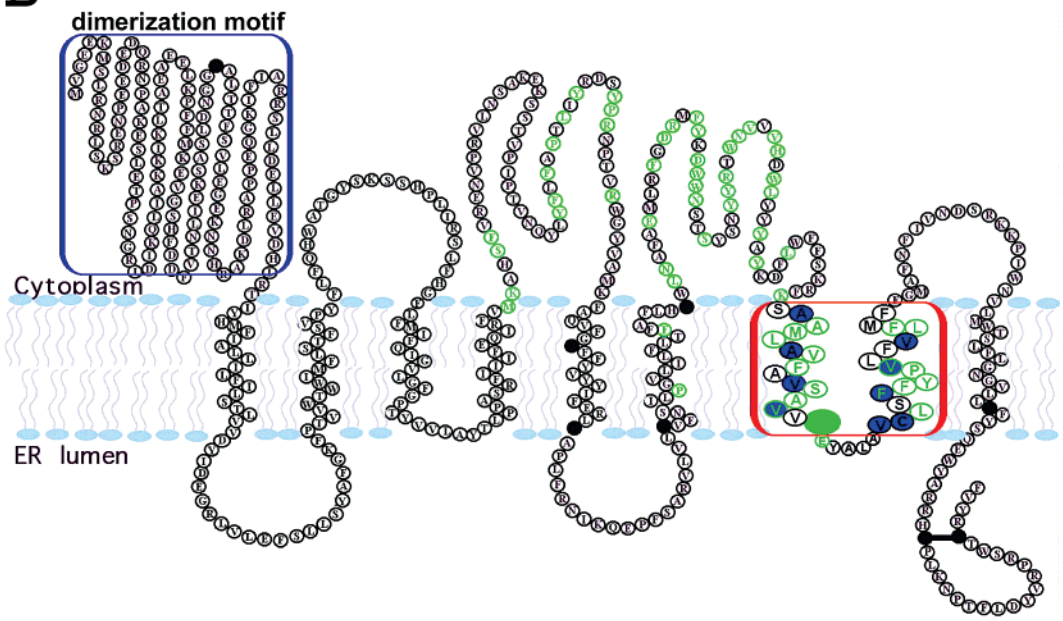

FIGURE 1: (A) Amino acid sequence of human ACAT1. Residues conserved in mammalian ACAT1, ACAT2, and DGAT1 are shown as green letters. (B) Nine-transmembrane-domain model for ACAT1, based on previous work (*10*). TMD7 and TMD8 are boxed by a red rectangle. Residues in TMD7 (S446−H460) and TMD8 (V466−F481) are shown as larger circles; the residues located at the subunit interaction surface as revealed in this work are shown as blue-filled circles. Native Cys are shown as black circles; the active-site His-460 within TMD7 is shown as a large solid green circle. The N-terminal domain responsible for dimerization of the ACAT1 dimer is boxed by a blue rectangle. In this work, a mutant ACAT1 (C2 ACAT1) in which all free Cys residues were replaced by alanines (C92A, C333A, C345A, C365A, C387A, C467A, and C516A) was used as the mutagenesis template.

that when TMD8 is placed as a helical wheel, the five reactive residues (V466C, A467C, F470C, V474C, and V477C) are all located at the same side of the coil. These residues may form a subunit interaction surface between two adjacent TMD8s. Other engineered mutants within TMD8 could not form detectable dimers. As shown in Figure 4B, except for F481, these residues are all located on the opposite side of the putative subunit interaction surface. We have shown earlier that, within TMD7 and TMD8, six mutants (M449C, F453C, S456C, A457C, H460C, and F479C) exhibited very low enzyme activity (Figure 2). When viewed in the helical wheel model (Figure 4), these residues are all located at the side opposite that of the putative subunit interaction surface within TMD7 or within TMD8.

Cross-Linking Efficiency of Cys in TMD7 and TMD8 Is Independent of ER Cholesterol Content. We asked if cholesterol content in the ER membrane may affect the reactivity of Cys in TMD7 and TMD8 toward CuP mediated cross-linking. To address this question, we developed a system that causes rapid change in cellular ER cholesterol

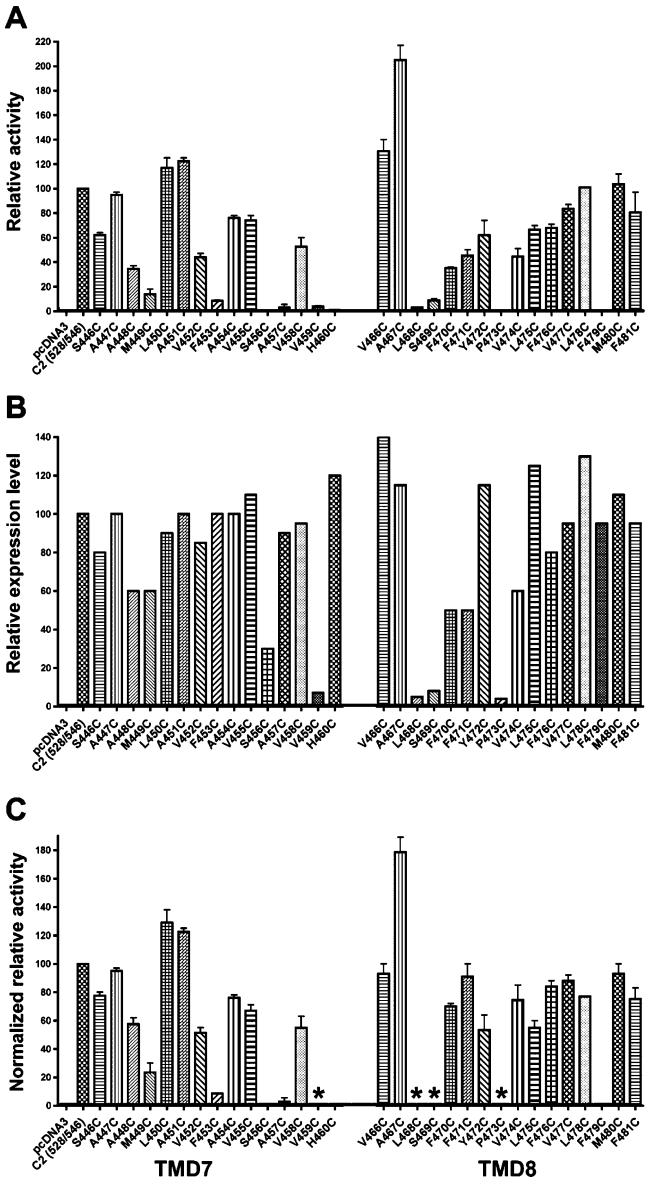

FIGURE 2: Enzymatic activities and protein expression levels of various single Cys mutant ACAT1s: (A) relative ACAT enzyme activities, (B) relative protein expression levels, and (C) normalized ACAT activities. The ACAT-deficient AC29 cells were transiently transfected with the vector (pcDNA3) only, or with the normal C2-(528/546) hACAT1 construct, or with various single Cys mutant ACAT1s constructs as indicated. ACAT1 protein expression was determined by procedures described under Experimental Procedures. For panels A and C, the dpm values of cells transfected with the pcDNA3 vector only were used as the blank value (250−300 dpm); the value found in cells expressing the normal C2(528/546) hACAT1 was used as the 100% value (1000−1500 dpm). Results shown are representative of two independent experiments. The asterisks indicate those mutant constructs with which the activity normalization could not be done, because their enzyme activities and expression levels were too low to be quantified.

content. We cultured transfected cells expressing normal C2 ACAT1 in cholesterol-rich or cholesterol-poor medium. The cholesterol-rich medium contained lipoproteins and additional cholesterol, delivered as cholesterol:methyl-β-cyclodextran complex; the cholesterol-poor medium was the lipoprotein-free medium, with mevinolin/mevalonate added to block endogenous sterol biosynthesis. Cells grown in these two media are expected to exhibit large differences in cholesterol content in various cellular membranes. It is difficult to purify various membranes, especially the ER membranes, to essential homogeneity. In fact, at present, direct methods that measure cholesterol content in the ER membranes are not available. ACAT1 is a resident enzyme in the ER; the ACAT activity in intact cells qualitatively reports the cellular cholesterol level in the ER (*8*). To test the efficacy of our procedure in changing the ER cholesterol content, we grew cells in cholesterol-rich or cholesterol-poor medium for 24 h and then measured their ACAT enzyme activity in intact cells. The results show that the ACAT activity of cells grown in cholesterol-rich medium is much higher than that of cells grown in cholesterol-poor medium (Figure 5A), while the ACAT1 protein expression levels of cells grown in these two different media did not change (Figure 5B). These results imply that cells grown in the cholesterol-rich medium contain higher ER cholesterol levels than those grown in the cholesterol-poor medium. With this procedure in place, we grew transfected cells that express various ACAT1 constructs in cholesterol-rich or cholesterol-poor medium, then prepared microsomes from these cells, and carried out disulfide cross-linking experiments. As shown in Figure 5C, regardless of the growth medium, the A448C, A454C, and H460C mutants exhibited no reactivity toward CuP, while the A447, A451C, V455C, V458C, V466C, A467C, and V477C mutants exhibited significant reactivity toward CuP. These results show that the reactivity of Cys located within TMD7 and TMD8 toward CuP is independent of the cholesterol content in the ER membrane.

Accessibility of Residues F453, A457, H460, and F479 to Small Molecules. The results described earlier (Figure 2) show that mutating any of the residues F453, A457, H460, and F479 to Cys did not seriously affect the structural integrity of the protein but caused severe loss in enzyme activity, suggesting that these four residues may play critical roles in enzyme catalysis and/or substrate binding. We wanted to compare the accessibility of these four residues toward various small molecules. To pursue this aim, we developed a two-step procedure. First, microsomes that contained various single Cys mutant ACAT1s were either untreated or treated with one of three small, cysteine-specific modification agents under nondenaturing conditions. The three reagents used were 4-acetamido-4′-maleimidylstilbene-2,2′-disulfonic acid (AMS), a hydrophilic, negatively charged reagent, MW 490; *N*-ethylmaleimide (NEM), a modestly hydrophobic reagent with no charge, MW 125; and *N*-phenylmaleimide (NPM), a very hydrophobic reagent with no charge, MW 173. Because their molecular weights are all relatively small, chemical modification by any one of the three reagents would not cause any detectable increase in the apparent MW of the modified ACAT1 on SDS−PAGE. After treatment with the small MW reagent, we carried out the second step by denaturing the microsomes with SDS and then treated the microsomes with poly(ethylene glycol)$_{5000}$−maleimide (PEG-mal), which is a specific cysteine-modifying agent with a much larger molecular weight. Modification by PEG-mal causes a detectable increase in the apparent MW of the ACAT1 band on SDS−PAGE (*16*). The alteration in the apparent MW of the ACAT1 band could be easily detected by performing western blotting after SDS−PAGE (*16*, *10*). We prepared microsomes expressing various single Cys ACAT1s and used the two-step procedure to compare the relative reactivity of various engineered Cys toward

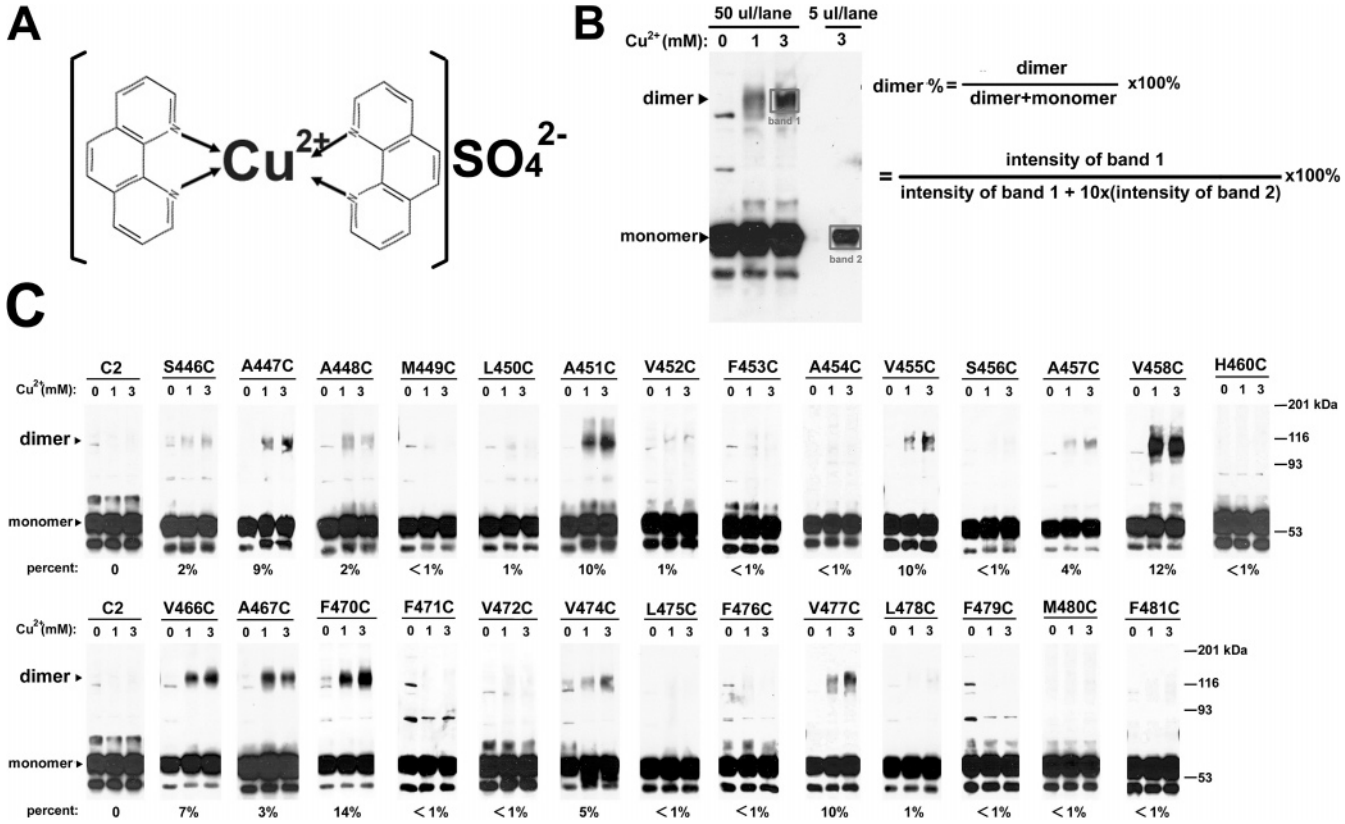

FIGURE 3: CuP oxidized disulfide cross-linkings of various single Cys ACAT1 mutants. (A) Structure of CuP. (B) Quantitation of cross-linking by CuP. Three sample lanes containing 50 μL of samples treated with CuP at 0, 1, or 3 mM are shown. In addition, a lane that contained 5 μL of the sample treated with 3 mM CuP was run in parallel. The gel was subjected to western blot analysis. The purpose of the last lane was to avoid the problem of signal saturation in western blotting. The method used to calculate the percentage of cross-linked hACAT1 dimer is shown to the right of the western blot data. (C) Cross-linkings of various mutant hACAT1s. Microsomes expressing various mutant ACAT1s (indicated at the top of each set) were treated with or without CuP at final concentrations as indicated. Analyses of the cross-linking data were described under Experimental Procedures. Percent cross-linking is based on the method described in panel B and is reported at the bottom of each lane. The results are the composite of several experiments. The exposure time for western analysis ranged from 30 s to 2 min. For each construct, the results shown are representative of at least two independent experiments.

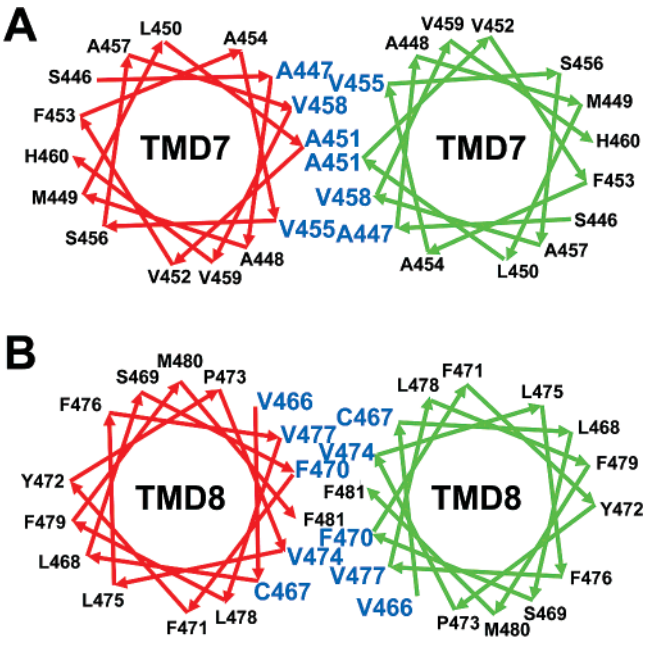

FIGURE 4: Helical wheels of (A) two TMD7s or (B) two TMD8s in dimeric ACAT1. One subunit is shown in red, and the other is shown in green. Letters in blue indicate residues located at the interface between the two TMD7s or between the two TMD8s.

AMS, NEM, and NPM in vitro; microsomes that contained the normal C2 ACAT1 were employed as a negative control. For each ACAT1 sample, we present the results in four lanes (Figure 6A): lane 1, without any small modification reagent; lane 2, AMS; lane 3, NEM; and lane 4, NPM. To analyze the data semiquantitatively, we introduced two parameters, designated as *R*1 and *R*2. *R*1 is the relative signal intensity of ACAT1 not modified by PEG-mal after treatment with AMS, NEM, or NPM as indicated. The *R*1 value reports the relative reactivity of a given Cys toward each of the three small modification reagents. *R*2 is the ratio of signal intensity of the PEG-mal-modified ACAT1 versus that of the non-PEG-mal-modified ACAT1 after NPM treatment. The *R*2 value reports the relative accessibility of a given Cys to NPM.

The results presented in Figure 6A show two characteristics: first, for each Cys residue, the *R*1 values ranged from 0 to 1 and the hydrophobic reagent NPM always gave the highest *R*1 value. Second, for TMD7, the residues located at the cytoplasmic side of the ER membrane—A447C, A448C, M449C, L450C, V452C, and F453C—are in general more accessible to modification; their *R*2 values were always 0:1. In contrast, the residues located at the lumenal side of the ER membrane—A454C, V455C, V458C, and H460C—are in general less accessible to modification; their *R*2 values ranged from 0.1:1 to 0.7:1. These results suggest that the

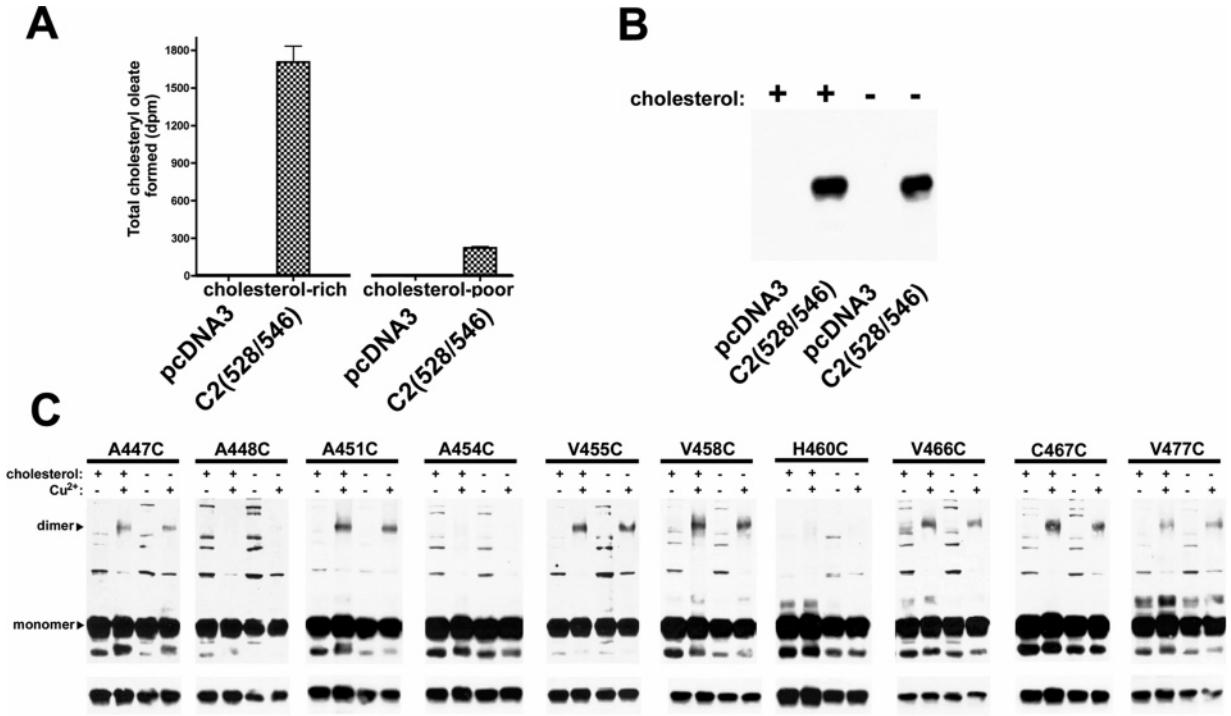

FIGURE 5: (A) ACAT activity in cells expressing normal C2 ACAT1 or pcDNA3 vector only. Cells were grown in cholesterol-rich or cholesterol-poor medium as indicated; media are described under Experimental Procedures. (B) ACAT1 protein expression level in cells expressing normal C2 ACAT1 or pcDNA3 vector only. Cells were grown in cholesterol-rich medium (+) or cholesterol-poor medium (−) as indicated. ACAT1 protein expression was determined by western blot as described under Experimental Procedures. (C) Oxidized disulfide cross-linkings of various mutant ACAT1s. Microsomes used as the ACAT1 source were isolated from cells grown in cholesterol-rich medium (+) or in cholesterol-poor medium (−) as indicated. DFisulfide cross-linking was performed as described under Experimental Procedures. The final concentration of CuP used was 3 mM. Signals of the ACAT1 monomer bands (shown at the bottom panel) were developed with shorter exposure time than those of the dimer bands (shown at the top panel).

hydrophobic reagent NPM penetrates the ER lipid bilayer more effectively than its less hydrophobic counterparts.

The residues in TMD8 located on either the lumenal side or the cytoplasmic side of the ER membrane were in general more resistant to modification, especially by the hydrophilic AMS. Two residues, L478C and F481C, showed significant resistance to modification by any of the small MW reagents employed, including NPM. It is possible that these two residues are located in a structurally sealed environment that is inaccessible to any small reagent. In TMD7, while F453C, A457, and H460 are all located at the lumenal segment, F453C and A457 were quite accessible to modification, especially toward NPM; in contrast, H460C was very resistant to modification. In TMD8, the Cys of the loss-of-activity residue F479C was accessible to small modification agents, especially hydrophobic ones. These results suggest that residues F453, A457, and F479 are located in relatively open region(s), while H460C is located in a much more compact and sealed region.

Inspection of results presented in lane 1 of Figure 6A reveal that, for most of the mutant ACAT1s, the engineered Cys were completely modified by PEG-mal; however, the Cys present in M449C, L450C, F453C, L478C, and F479C could not be completely modified by PEG-mal. These results suggest that the Cys at these positions might have been partially modified by a certain sulfhydryl-modifying molecule-(s), such as glutathione (GSH) and/or cysteine, prior to modification by PEG-mal. To determine whether the partial modifications of these Cys occur in intact cells or in vitro, we performed quick lysis of cells that express the various Cys ACAT1 mutants in a solution that contain 10% SDS and 4 mM PEG-mal. The results (Figure 6B) show that the single Cys present in the M449C, L450C, F453C, L478C, and F479C ACAT1 mutants still could not be completely modified by PEG-mal. In contrast, the Cys present in the H460C mutant (serving as a negative control) was completely modified by PEG-mal, suggesting that the engineered Cys present in M449C, L450C, F453C, L478C, and F479C ACAT1s are partially modified by GSH/cysteine in intact cells prior to cell lysis.

DISCUSSION

In this work, we used the catalytically active C2 ACAT1 as the template, performed Cys-scanning mutagenesis within TMD7 (aa 446−460) and TMD8 (aa 466−481), expressed each of these mutant ACAT1s in a CHO cell line lacking endogenous ACAT1 (AC29), and measured their enzyme activities. We also used the Cu(1,10-phenanthroline)$_2$SO$_4$-(CuP-) mediated oxidative disulfide cross-linking method to probe possible interactions between the two adjacent TMD7s and the two adjacent TMD8s. The results show that each of the five mutants F453C, S456C, A457C, H460C, and F479C had extremely low normalized enzymatic activities. The protein expression levels of the F453C, A457C, H460C, and F479C mutations are essentially normal, suggesting that mutations at F453, A457, H460, and F479 do not seriously affect the structural integrity. Previous work showed that mutations of the conserved His in the membrane-bound acyltransferase family (H460 in hACAT1) caused severe inactivation of enzyme activities in ACAT1 or ACAT2 (*10*, *5*). Our work shows that, in addition to H460, residues F453, A457, and F479 may also be essential to provide optimal

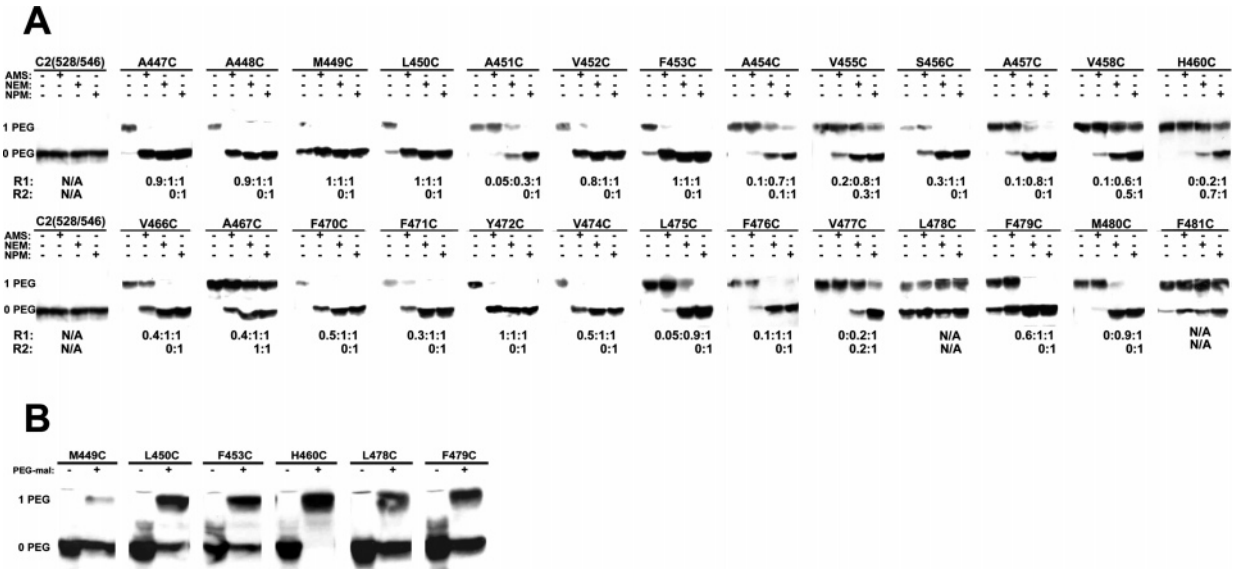

FIGURE 6: (A) Comparison of the modification efficiency of three small sulfhydryl-reactive reagents, AMS, NEM, and NPM. (B) Rapid chemical modification by PEG-mal under denaturing conditions. In panel A, the supernatants of the lysates of cells expressing various mutant ACAT1 as indicated were treated with NEM, AMS, or NPM (at 4 mM concentration) at 0 °C for 1 h. Afterward, the excess NEM, AMS, or NPM was quenched by adding 2-mercaptoethanol. The free Cys not reacting with the small sulfhydryl-reactive reagent under native conditions were modified by PEG-mal (at 5 mM) by performing the PEG-mal modification under denatured condition (5% SDS). Definitions for parameters R1 and R2 are described in the text. L478C and F481C were resistant to modification by any of the three small modification reagents; therefore, their R1 and R2 are labeled as N/A. In panel B, CHO cells transiently expressing various mutant ACAT1s as indicated were cultured in 6-well plates and directly lysed by adding 200 μL of lysate buffer (10% SDS, 50 mM Tris-HCl, and 1 mM EDTA, pH 7.5) containing 4 mM PEG-mal. The modification was carried out at room temperature for 30 min. Mixtures were analyzed by SDS−PAGE, and ACAT1 bands were visualized by western blot with anti-ACAT1 antibodies. Results are representative of two independent experiments.

enzyme catalysis and/or substrate binding. F453 and A457 are conserved in mammalian ACAT1, ACAT2, and DGAT1; the F479 residue is conserved in mammalian ACAT1 and ACAT2. Other data show that the normalized enzyme activities of the S456C and M449C mutant ACAT1s are very low, but their protein expression levels are also very low; therefore, we are less certain about the roles of S456 or M449 in the catalytic actions of the enzyme.

Coiled-coils are gently twisted, ropelike bundles, containing 2−5 α-helices in parallel or antiparallel configuration. They contain repeats of seven residues, with the first and fourth residues generally occupied by a hydrophobic amino acid (*21*). They form the dominant force to produce the oligomerization domain in several integral membrane proteins that have been rigorously examined (*22*). The results described in this work show that in TMD7 there are four residues (A447C, A451C, V455C, and V458C) very reactive to CuP. The helical wheel analysis demonstrates that these four Cys are all located at one side of the coil. These four single Cys mutants all retained high ACAT enzymatic activity and normal protein expression levels. The same situation holds true for the five mutants V466C, A467C, F470C, V474C, and V477C in TMD8. Together, these results suggest that the single C substitution in any of these residues did not significantly alter the structure of the enzyme. In TMD7, the natural residues located at these positions are composed of two Ala and two Val. In TMD8, the natural residues at these positions are composed of three Val. Overall, these results are consistent with the interpretation that TMD7 and TMD8 form coiled-coils and that the aliphatic hydrophobic amino acids located at one side of the coils, Val in particular, form the subunit interface between the two adjacent TMD7s and the two adjacent TMD8s. The F481C mutant is nonreactive to CuP. It is within the interaction surface of TMD8 but located at the cytosolic end of the coil. This result suggests that the two TMD8s may be nonparallel; the cytosolic ends of TMD8s from two subunits may be far from each other. Our present data cannot determine whether residues in TMD7 in one subunit may also interact with residues in TMD8 in the other subunit. This possibility requires further investigation. We had previously identified a subunit interaction site near the N-terminal domain of ACAT1 (*11*). The subunit interaction surface in the two adjacent TMD7s and TMD8s described in this work may contribute to form the second dimerization domain; however, this domain may involve additional structural motif(s), and further investigations are needed in order to test this possibility.

We used the oxidative cross-linking strategy to test whether the CuP-induced dimer formation might be affected by cellular cholesterol loading. The results obtained suggest that the subunit interaction between two TMD7s and two TMD8s is independent of cholesterol content in the ER. The helical wheel analysis shows that, within the TMD7 and TMD8 coils, the six single Cys mutants exhibiting severe loss in enzyme activity are all located at the side opposite the subunit interaction surface. This analysis suggests that the two sides of TMD7 and of TMD8 fulfill two distinct functions: one side is involved in subunit interactions, and residues involved in subunit interaction are not involved in enzymatic actions. In contrast, several residues located in the other side, including F453C, A457C, H460C, and F479, are involved in enzyme catalysis. We performed additional experiments to probe the microenvironments of these four residues. The results suggest that residues F453, A457, and F479 are located in relatively open region(s); they are

accessible to small molecules. In contrast, H460C is located at a compact region; it is inaccessible to small molecules. Recently, X-ray crystal structures of several water soluble proteins involved in binding cholesterol have become available (*23*−*27*). A common feature of these studies is the presence of a central, sequestered hydrophobic tunnel involved in binding the cholesterol moiety. On the basis of this analogy, we speculate that residues F453, A457, and F479 may be part of a lipid binding tunnel that interacts with the hydrophobic part of cholesterol, while residue H460 may interact with the 3-β-OH moiety of the sterol and serve as a general base in catalysis, as discussed previously (*10*). We are currently developing various biochemical assays to test this possibility.

ACKNOWLEDGMENT

We thank Helina Josephson for careful editing of the manuscript.

REFERENCES

1. Chang, T. Y., Chang, C. C. Y., and Cheng, D. (1997) Acyl-coenzyme A:cholesterol acyltransferase, *Annu. Rev. Biochem. 66*, 613−638.
2. Chang, T. Y., Chang, C. C. Y., Lin, S., Yu, C., Li, B. L., and Miyazaki, A. (2001) Roles of acyl-coenzyme A:cholesterol acyltransferase-1 and -2, *Curr. Opin. Lipidol. 12*, 289−296.
3. Rudel, L., Lee, R., and Cockman, T. (2001) Structure, function, and regulation of ACAT, *Curr. Opin. Lipidol. 12*, 121−127.
4. Song, B. L., Wang, C. H., Yao, X. M., Yang, L., Zhang, W. J., Wang, Z. Z., Zhao, X. N., Yang, J. B., Qi, W., Yang, X. Y., Inoue, K., Lin, Z. X., Zhang, H. Z., Kodama, T., Chang, C. C., Liu, Y. K., Chang, T. Y., and Li, B. L. (2006) Human acyl-CoA: cholesterol acyltransferase 2 gene expression in intestinal Caco-2 cells and in hepatocellular carcinoma, *Biochem. J. 394*, 617−626.
5. Lin, S., Lu, X., Chang, C. C. Y., and Chang, T. Y. (2003) Human Acyl-Coenzyme A:cholesterol acyltransferase 2 (hACAT2) expressed in Chinese hamster ovary cells: membrane topology and active site location, *Mol. Biol. Cell 14*, 2447−2460.
6. Horton, J. D., Goldstein, J. L., and Brown, M. S. (2002) SREBPs: activators of the complete program of cholesterol and fatty acid synthesis in the liver, *J. Clin. Invest. 109*, 1125−1131.
7. Chang, T. Y., Chang, C. C., Ohgami, N., and Yamauchi, Y. (2006) Cholesterol sensing, trafficking, and esterification, *Annu. Rev. Cell Dev. Biol. 22*, 129−157.
8. Liu, J., Chang, C. C., Westover, E. J., Covey, D. F., and Chang, T. Y. (2005) Investigating the allosterism of acyl coenzyme A:cholesterol acyltransferase (ACAT) by using various sterols: In vitro and intact cell studies, *Biochem. J. 391*, 389−397.
9. Yu, C., Chen, J., Lin, S., Liu, J., Chang, C. C. Y., and Chang, T. Y. (1999) Human acyl-CoA:cholesterol acyltransferase-1 is a homotetrameric enzyme in intact cells and in vitro, *J. Biol. Chem. 274*, 36139−36145.
10. Guo, Z. Y., Lin, S., Heinen, J. A., Chang, C. C., and Chang, T. Y. (2005) The active site His-460 of human acyl-coenzyme A:cholesterol acyltransferase 1 resides in a hitherto undisclosed transmembrane domain, *J. Biol. Chem. 280*, 37814−37826.
11. Yu, C., Zhang, Y., Lu, X., Chang, C. C. Y., and Chang, T. Y. (2002) The role of the N-terminal hydrophilic domain of acyl coenzyme A:cholesterol acyltransferase 1 on the enzyme's quaternary structure and catalytic efficiency, *Biochemistry 41*, 3762−3769.
12. Falke, J. J., and Koshland, D. E., Jr. (1987) Global flexibility in a sensory receptor: a site-directed cross-linking approach, *Science 237*, 1596−1600.
13. Kawasaki-Nishi, S., Nishi, T., and Forgac, M. (2003) Interacting helical surfaces of the transmembrane segments of subunits a and c′ of the yeast V-ATPase defined by disulfide-mediated cross-linking, *J. Biol. Chem. 278*, 41908−41913.
14. Flanagan, J. J., and Barlowe, C. (2006) Cysteine-disulfide cross-linking to monitor SNARE complex assembly during endoplasmic reticulum-Golgi transport, *J. Biol. Chem. 281*, 2281−2288.
15. Chang, C. C. Y., Chen, J., Thomas, M. A., Cheng, D., Del Priore, V. A., Newton, R. S., Pape, M. E., and Chang, T. Y. (1995) Regulation and immunolocalization of acyl-coenzyme A:cholesterol acyltransferase in mammalian cells as studied with specific antibodies, *J. Biol. Chem. 270*, 29532−29540.
16. Guo, Z. Y., Chang, C. C., Lu, X., Chen, J., Li, B. L., and Chang, T. Y. (2005) The disulfide linkage and the free sulfhydryl accessibility of acyl-coenzyme A:cholesterol acyltransferase 1 as studied by using mPEG5000-maleimide, *Biochemistry 44*, 6537−6546.
17. Cadigan, K. M., Heider, J. G., and Chang, T. Y. (1988) Isolation and characterization of Chinese hamster ovary cell mutants deficient in acyl-coenzyme A:cholesterol acyltransferase activity, *J. Biol. Chem. 263*, 274−282.
18. Sugii, S., Lin, S., Ohgami, N., Ohashi, M., Chang, C. C., and Chang, T. Y. (2006) Roles of endogenously synthesized sterols in the endocytic pathway, *J. Biol. Chem. 281*, 23191−23206.
19. Chang, C. C. Y., Doolittle, G. M., and Chang, T. Y. (1986) Cycloheximide sensitivity in regulation of acyl coenzyme A:cholesterol acyltransferase activity in Chinese hamster ovary cells. I. Effect of exogenous sterols, *Biochemistry 25*, 1693−1699.
20. Chang, T. Y., Limanek, J. S., and Chang, C. C. Y. (1981) A simple and efficient procedure for the rapid homogenization of cultured animal cells grown in monolayer, *Anal. Biochem. 116*, 298−302.
21. Muller, K. M., Arndt, K. M., and Alber, T. (2000) Protein fusions to coiled-coil domains, *Methods Enzymol. 328*, 261−282.
22. Arkin, I. T. (2002) Structural aspects of oligomerization taking place between the transmembrane alpha-helices of bitopic membrane proteins, *Biochim. Biophys. Acta. 1565*, 347−363.
23. Tsujishita, Y., and Hurley, J. H. (2000) Structure and lipid transport mechanism of a StAR-related domain, *Nat. Struct. Biol. 7*, 408−414.
24. Friedland, N., Liou, H. L., Lobel, P., and Stock, A. M. (2003) Structure of a cholesterol-binding protein deficient in Niemann-Pick type C2 disease, *Proc. Natl. Acad. Sci. U.S.A. 100*, 2512−2517.
25. Ko, D. C., Binkley, J., Sidow, A., and Scott, M. P. (2003) The integrity of a cholesterol-binding pocket in Niemann-Pick C2 protein is necessary to control lysosome cholesterol levels, *Proc. Natl. Acad. Sci. U.S.A. 100*, 2518−2525.
26. Im, Y. J., Raychaudhuri, S., Prinz, W. A., and Hurley, J. H. (2005) Structural mechanism for sterol sensing and transport by OSBP-related proteins, *Nature 437*, 154−158.
27. Chang, C. C., Lee, C. Y., Chang, E. T., Cruz, J. C., Levesque, M. C., and Chang, T. Y. (1998) Recombinant acyl-CoA:cholesterol acyltransferase-1 (ACAT-1) purified to essential homogeneity utilizes cholesterol in mixed micelles or in vesicles in a highly cooperative manner, *J. Biol. Chem. 273*, 35132−35141.

BI7011367